

## RESEARCH ARTICLE

# Bone without minerals and its secondary mineralization in Atlantic salmon (*Salmo salar*): the recovery from phosphorus deficiency

P. Eckhard Witten<sup>1,\*</sup>, Per Gunnar Fjellidal<sup>2</sup>, Ann Huysseune<sup>1</sup>, Charles McGurk<sup>3</sup>, Alex Obach<sup>3</sup> and Matthew A. G. Owen<sup>3</sup>

## ABSTRACT

Calcium and phosphorus (P) are the main bone minerals, and P deficiency can cause hypomineralized bones (osteomalacia) and malformations. This study used a P-deficient salmon model to falsify three hypotheses. First, an extended period of dietary P deficiency does not cause pathologies other than osteomalacia. Second, secondary mineralization of non-mineralized bone is possible. Third, secondary mineralization can restore the bones' mineral composition and mechanical properties. For 7 weeks, post-smolt Atlantic salmon (*Salmo salar*) received diets with regular P content (RP) or with a 50% lowered P content (LP). For additional 9 weeks, RP animals continued on the regular diet (RP-RP). LP animals continued on the LP diet (LP-LP), on a regular P diet (LP-RP) or on a high P diet (LP-HP). After 16 weeks, animals in all groups maintained a non-deformed vertebral column. LP-LP animals continued bone formation albeit without mineralization. Nine weeks of RP diet largely restored the mineral content and mechanical properties of vertebral bodies. Mineralization resumed deep inside the bone and away from osteoblasts. The history of P deficiency was traceable in LP-RP and LP-HP animals as a ring of low-mineralized bone in the vertebral body endplates, but no tissue alterations occurred that foreshadow vertebral body compression or fusion. Large quantities of non-mineralized salmon bone have the capacity to re-mineralize. If 16 weeks of P deficiency as a single factor is not causal for typical vertebral body malformations, other factors remain to be identified. This example of functional bone without minerals may explain why some teleost species can afford to have an extremely low mineralized skeleton.

**KEY WORDS:** Teleost skeleton, Vertebral column, Bone growth, Skeletal malformation, Notochord

## INTRODUCTION

The bone of vertebrates is a composite material. The main components are a type I collagen-based matrix and minerals, primarily calcium (Ca) and phosphorus (P). Consequently, skeletal health depends on sufficient Ca and P intake. Insufficient P intake or impaired uptake causes hypomineralized bones, also known as osteomalacia (Weisberg et al., 2004). In humans, insufficient dietary P supply is rare (Knochel, 1977), but a lack of vitamin D is


known to reduce Ca and P uptake in the gut and increases renal P excretion, leading to the condition known as rickets (Antonucci et al., 2018). P uptake disorders can also relate to the aberrant actions of fibroblast growth factor 23 (FGF23), an osteoblast- and osteocyte-released hormone that stimulates renal P excretion (Hori et al., 2011). Hypophosphatasia is another low-P condition, a heritable reduced activity of tissue-nonspecific alkaline phosphatase (Goetz et al., 2010; Bloch-Zupan, 2016). In human children, under-mineralized bones, owing to P deficiency, are soft and become malformed (Weisberg et al., 2004). Also, the P uptake of teleost fish is vitamin D dependent. Fjellidal et al. (2016) and Smedley et al. (2018) present data that point to a FGF23 function in Atlantic salmon similar to its function in mammals. The primary source of vitamin D in the aquatic food chain is vitamin D-rich plankton. Teleosts store vitamin D in the liver, and diets for farmed fish are enriched with vitamin D (Lock et al., 2010; Darias et al., 2011). Thus, teleosts do not suffer from rickets. However, it is known that farmed salmon can suffer from insufficient P intake if diets do not contain enough P, or if the dietary P source is indigestible. The latter can be the case if fish meal is the primary P source in the diet (Albrektsen et al., 2009).

In farmed salmonids, skeletal deformities affecting the vertebral column have been related to dietary P deficiency, such as vertebral body compression, vertebral body fusion, abnormal bone softness, structural distortions including curled ribs and undersized vertebral bodies (Baeverfjord et al., 1998; Sullivan et al., 2007a,b; Deschamps et al., 2008; Fjellidal et al., 2012a; Poirier Stewart et al., 2014). Moreover, hyper radio-dense vertebral bodies have been linked to P deficiency (Helland et al., 2006). Teleost vertebral bodies are composed of vertebral centra and associated structures (arches, spines and ribs), described in detail for Pacific salmon (De Clercq et al., 2017). Centra consist of two conical vertebral body endplates (horizontal hourglass), spongy bone between the endplates and notochord tissues in the intervertebral space (Laerm, 1976) (Fig. 1). Given the many vertebral column pathologies that are assumed to be linked to insufficient dietary P supply, Witten et al. (2016) investigated the primary bone pathology caused by a P-deficient diet. In that study, Atlantic salmon in the early seawater phase (post-smolts) were exposed to severe dietary P deficiency for 10 weeks. The animals developed severe osteomalacia but did not show bone deformities, structural changes of the bone matrix or aberrations of bone cells. Bones continued to grow normally, although new bone matrix was completely devoid of minerals. X-rays suggested the presence of undersized vertebral bodies, but further analysis revealed regular amounts of non-mineralized, radio-translucent bone matrix. The experiment demonstrated uncoupling of bone formation and bone mineralization but failed to reveal a primary P-deficiency-related bone pathology, other than osteomalacia. The lack of skeletal malformations was a surprising outcome of that study. This elicited

<sup>1</sup>Ghent University, Biology Department, Ledeganckstraat 35, 9000 Ghent, Belgium.

<sup>2</sup>Institute of Marine Research (IMR), Matre Aquaculture Research Station, N-5984, Matredal, Norway. <sup>3</sup>Skretting Aquaculture Research Centre, P. O. Box 48, N-4001, Stavanger, Norway.

\*Author for correspondence (peckhardwitten@aol.com)

 P.E.W., 0000-0002-2928-5762

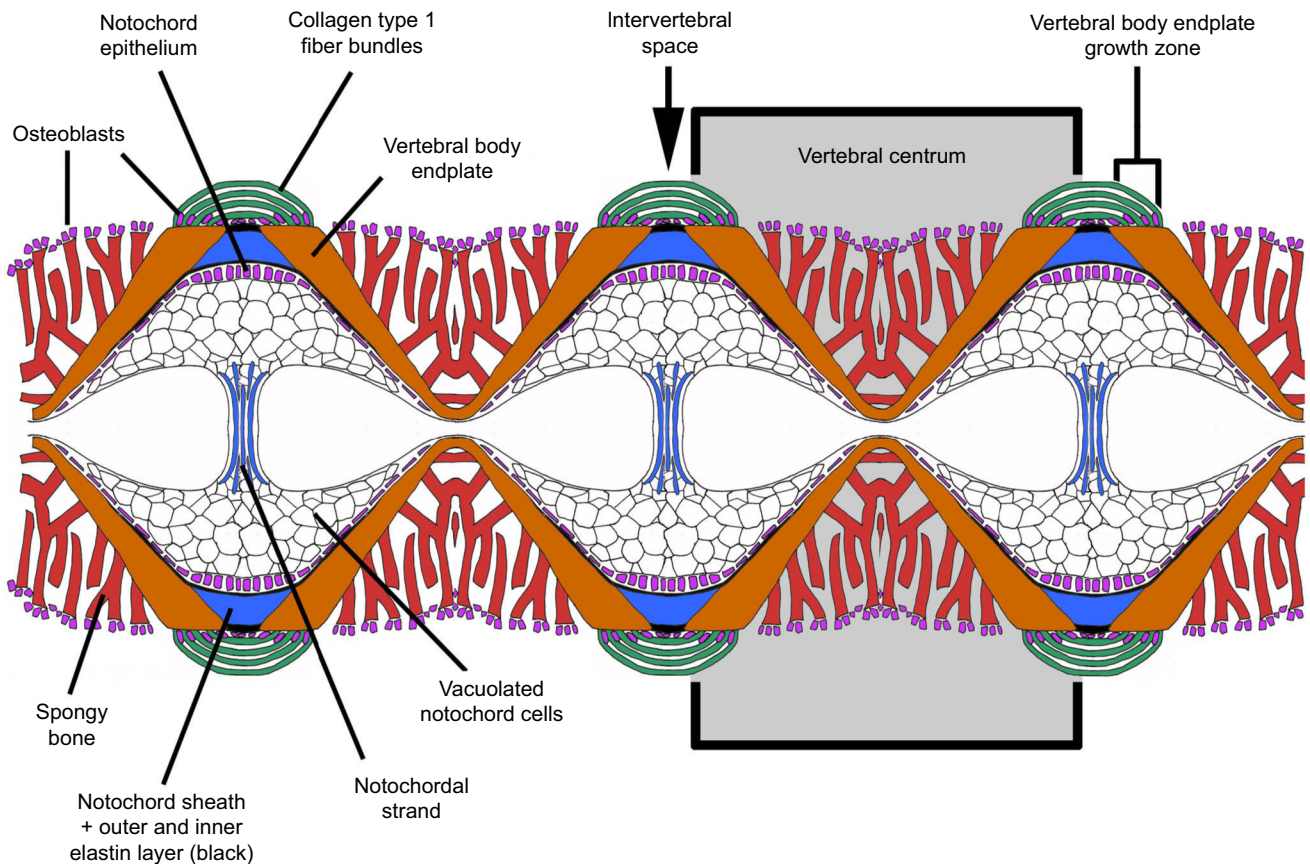


**Fig. 1. Schematic description of the internal structures of salmon vertebral centra, sagittal view.** Teleost vertebral centra have no cartilaginous precursors. Segmental mineralization of the notochord sheath (chordacentra) and intramembranous bone formation around the notochord (autocentra) establish the vertebral centra and thus the vertebral body endplates (Huxley, 1859; Arratia et al., 2001). The cells of the notochord epithelium (also named chordoblasts) secrete the collagen type 2 based notochord sheath. The sheath expands in the intervertebral spaces (Bensimon-Brito et al., 2012). Bone growth follows this expansion, which creates the typical amphicoelous (hourglass) shape of vertebral body endplates (Nordvik et al., 2005). Vertebrae are interconnected by the notochord sheath and by type 1 collagen fiber bundles outside the notochord (Gistelincx et al., 2018). Inside, vacuolated notochord cells and central fibers of the notochordal strand form a compressible cushion (Schmitz, 1998). Osteoblasts that expand the vertebral body endplates are located between the collagen type 1 fiber bundles. Trabeculae of the spongy bone that connect the vertebral body endplates initially also arise by intramembranous bone formation. Their structure and orientation is controlled by the direction of mechanical load (Laerm, 1976).

a study taking advantage of the salmon bone P-deficiency model to falsify the following hypotheses: (1) an extended period of dietary P deficiency will not generate skeletal pathologies other than osteomalacia; (2) it is possible to rescue the P-deficient bone phenotype with a P-sufficient diet; and (3) secondary mineralization can restore the mineral composition and the mechanical properties of previously non-mineralized bone. The dietary phosphorus levels used for the requirement P diets reflect the known nutrient requirements of Atlantic salmon (National Research Council, 2011) as formulated by Skretting, a global fish feed manufacturer. The low P and high P diets represent 50% and 150% of those defined requirements, respectively.

## MATERIALS AND METHODS

### Feeding experiment

The experiment was performed at Lerang Research Station (Skretting ARC, Lerang, Forsand, Norway). The experiment was conducted according to Norwegian legislation and approved by the Norwegian Animal Research Authority (NARA/FDU). All samplings were performed by scientists accredited by the Federation of Laboratory Animal Science Associations (FELASA). Atlantic salmon (*Salmo salar* Linnaeus 1758) eggs were obtained from

Erfjord Stamfisk (Salmobreed strain, Erfjord Stamfisk A/S, Erfjord, Norway) and hatched and reared in-house. Prior to the experiment fish were held in 1 m diameter tanks and fed a commercial standard diet Skretting Spirit 75, pellet size 3 mm (Skretting, Stavanger, Norway). The experiment started after the animals' seawater transfer (post-smolts), when their average mass was  $151.7 \pm 4.3$  g.

The design of the experiment is outlined in Fig. 2A. At the start of the experiment, 270 animals were anesthetized (MS-222, Sigma-Aldrich) and evenly distributed into nine 1 m diameter tanks supplied with a constant flow of clean seawater (salinity= $33.9 \pm 0.2$  ppt, temperature= $11.9 \pm 0.2^\circ\text{C}$ , oxygen= $103 \pm 1.6\%$ ). The fish were fed to apparent satiation twice a day; feed intake was monitored throughout the experiment, and waste feed was collected. For the duration of the experiment, the fish were kept in constant artificial light (photoperiod=24 h:0 h light:dark), a procedure used on farms to optimize food intake in Atlantic salmon (Berge et al., 2009; Imsland et al., 2014). For the initial 7 weeks, triplicate tanks of fish were fed one of two iso-nitrogenous, iso-caloric diets (Table S1): a P-sufficient diet (three tanks) formulated to have a total P content of 0.84% (regular P, RP), or a P-deficient diet (six tanks) with a total P of 0.47% (low P, LP) (Table S1). All diets were extruded via a Wenger twin screw extruder at the Feed Trial Plant, Skretting ARC,

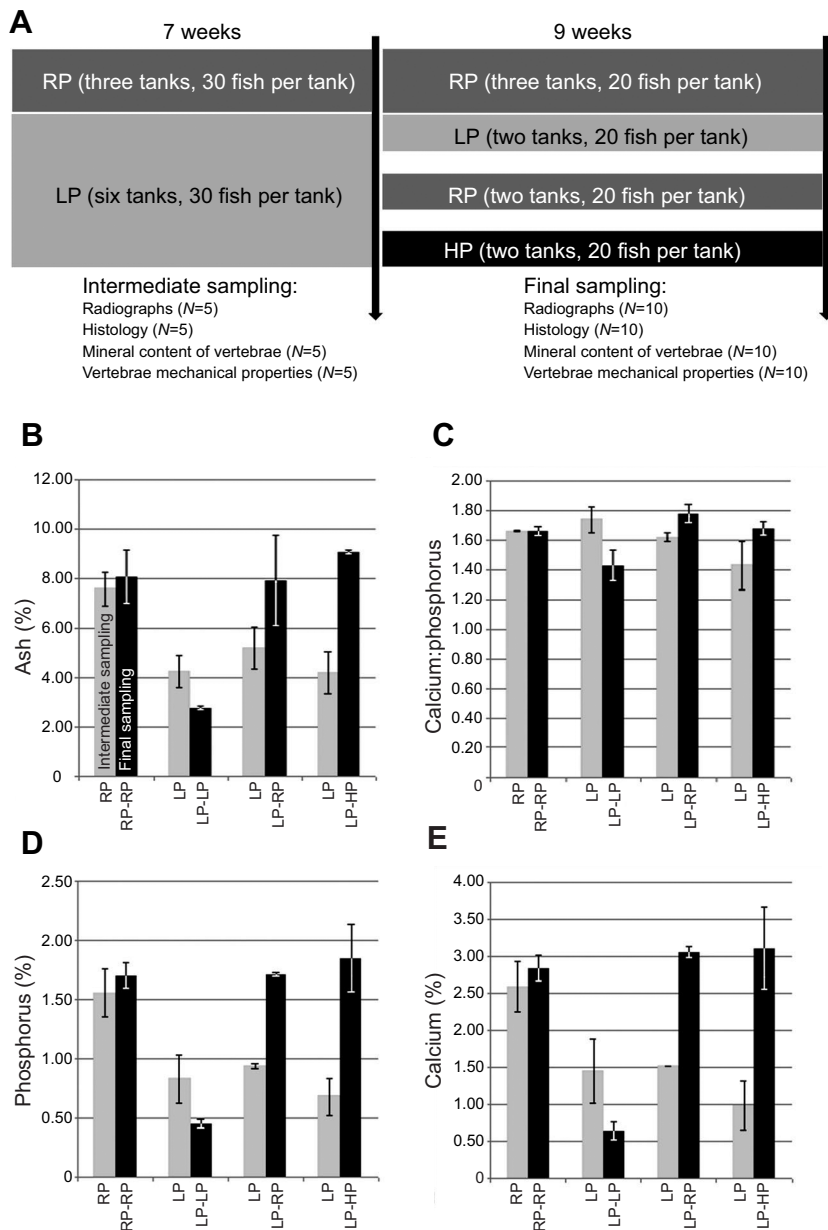


**Fig. 2. Experimental setup and mineral analysis.** (A) Setup of the experiment. RP, LP and HP indicate the phosphorus content of the diet – regular, low and high, respectively. Numbers at intermediate sampling and final sampling refer to the number of specimens examined per tank. (B–E) Mean±s.d. percentage dry mass of measured ash (B), calcium to phosphorus ratio (C), phosphorus (D) and calcium (E) content in vertebral bodies from the two experimental groups of Atlantic salmon (*Salmo salar*) after 7 weeks (gray columns) and after 16 weeks (final sampling, black columns). Note that after 16 weeks there is no significant difference between all RP-RP, LP-RP and LP-HP values but a significant difference from LP-LP values.

Stavanger, Norway. After 7 weeks, 10 animals were removed from each tank and sampled for radiographs, mineral content of whole fish and selected tissues, and for histology. Animals fed the RP diet continued on the same diet for a further 9 weeks (Fig. 2A). The six replicate tanks fed the LP diet for the initial 7 weeks either continued on the LP diet or were then fed either the RP diet or a high P diet (HP, total P content of 1.46%) (two tanks per diet group, Fig. 2A). These diets represent 100%, 50% and 150%, respectively, of dietary P requirements for Atlantic salmon (National Research Council, 2011). The experimental groups in the first phase of the experiment (weeks 0–7) were therefore RP and LP. In the second phase of the experiment (weeks 8–16), the experimental groups were RP-RP, LP-LP, LP-RP and LP-HP.

After a total experimental period of 16 weeks, all remaining fish were sampled. All fish were euthanized with an overdose of the anesthetic MS-222 (Sigma-Aldrich) and subsequently weighed and measured. The lateral and abdominal musculature was removed (filleted), after which the vertebral column was immediately

radiographed (see below) and then fixed in 10% neutral buffered formalin. Table S2 provides the data about the animals' mass, fork length, specific growth rate (SGR), feed conversion ratio (FCR) and condition factor ( $K$ ). The FCR was calculated as the total feed intake divided by the body mass gain and adjusted to account for mortality and uneaten food (National Research Council, 2011). The SGR (% increase in body mass per day) was calculated according to the following equation:  $SGR = [\ln(M_{bf}) - \ln(M_{bi})] / t \times 100$ , where  $M_{bi}$  is the initial body mass,  $M_{bf}$  is the final body mass and  $t$  is time (days).  $K$  was calculated by dividing the body mass (g) of the fish by the cube of the standard length (cm) (Froese, 2006).

#### Statistical analysis

Unless otherwise stated, all data are presented as means±s.d. All data were analyzed using GraphPad Prism 5.0 for Windows ([www.graphpad.com/scientific-software/prism](http://www.graphpad.com/scientific-software/prism)) with percent-age data arc-sine transformed before subsequent analysis. The statistical tests used are indicated next to the relevant data table or figure legend.

### Radiology

All fish were X-rayed using a Geirth XMF80 emitter and AGFA Structurix D4DW film. The X-ray unit was set to 80 kV, 15 mA and 4 s exposure at a distance of 80 cm between the X-ray tube and the film. Radiographs were developed according to the protocol of the manufacturer and digitized at 1200 dpi with a Heidelberg transparency scanner (Linoscan-1400). Details from X-rays were digitized at 4000 dpi with a Polaroid SprintScan 120 film scanner. The height and the length of vertebral bodies (radio-dense area) and the length of the intervertebral space (radio-translucent area) were measured on digitized radiographs using ImageJ software (<http://rsbweb.nih.gov/ij/download.html>). Ten individual vertebral bodies (33–42) from 20 individuals from each experimental group were measured. Measurements were taken after 7 weeks (RP and LP groups) and after 16 weeks (RP-RP, LP-LP, LP-RP and LP-HP groups).

### Whole-mount staining with Alizarin Red S

Complete vertebral bodies were stained according to the following protocol: 100% acetone (2×24 h); 100% ethanol (2×24 h); ethanol: water solutions to bring the vertebral bodies stepwise to water; 3% H<sub>2</sub>O<sub>2</sub> in 1% KOH (2 h); saturated Na-tetraborate (12 h); 0.1% Alizarin Red S in 1% KOH (12 h); 1% KOH glycerol solutions to bring the vertebral bodies into 100% glycerol (5 steps, 48 h each). A Zeiss Axio Zoom V16 Fluorescence Stereo Zoom Microscope with oblique illumination was used to visualize mineralized and non-mineralized bone matrix.

### Histology

Spine samples from vertebrae 32–36 were decalcified in a 10% EDTA solution and embedded in Paraplast. Serial sections of 5 µm thickness were prepared in the sagittal plane. Vertebrae 37–41 from each animal were not decalcified and were sectioned on a cryotome to visualize minerals. Paraffin sections were stained with Masson's trichrome and Azan for general connective tissue histology. Alcian Blue–hematoxylin staining was used to detect cartilage matrix (Witten and Hall, 2002). Von Kossa/Van Gieson stains were used to distinguish mineralized from non-mineralized bone (Presnell and Schreiber, 1998) on cryotome sections. A Zeiss Axio Imager-Z1 and a Leitz Dialux 22EB microscope, equipped with 5 MP CCD cameras, were used for analysis and documentation.

### Mechanical strength of single vertebrae

Vertebrae numbers 29–31 were dissected from fish of all groups obtained at the final sampling. The neural and hemal arches were removed, and the amphicoelous centra were used for mechanical testing and subsequent measurement of mineral content. The vertebrae were compressed in cranial-caudal direction using a texture analyser (TA-T2 Texture Analyser; Stable Micro Systems, Haslemere, UK) with a steadily advancing piston (6 mm min<sup>-1</sup>). The test was terminated when the vertebrae were 60% compressed in their cranial-caudal lengths. Load–deformation data were used to calculate stiffness (Fjellidal et al., 2004) which is equivalent to Young's modulus of elasticity (Currey, 2003). Resulting load–deformation data were continuously recorded. Results are presented as means±s.e.m. The biomechanical data used are based on mean values; in total, three vertebrae were measured per individual. The data were analyzed using Statistica version 13 (StatSoft, Tulsa, OK, USA). Potential effects of dietary P on vertebra stiffness were tested for using two-way nested ANOVA, with tank as random factor nested in diet group. Significant nested ANOVA results were

followed up by Student–Newman–Keuls (SNK) tests for *post hoc* comparison in order to detect differences between treatment groups.  $P < 0.05$  was regarded as significant.

### Mineral analysis of bones

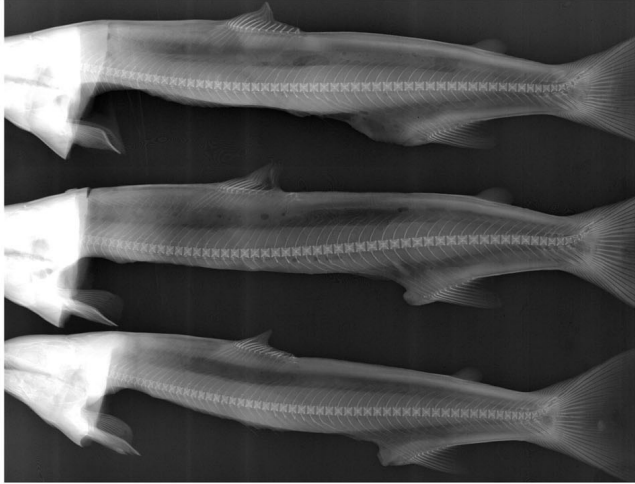
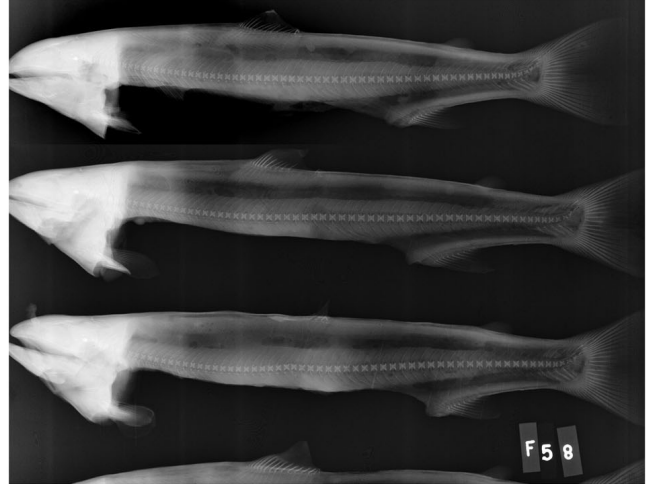
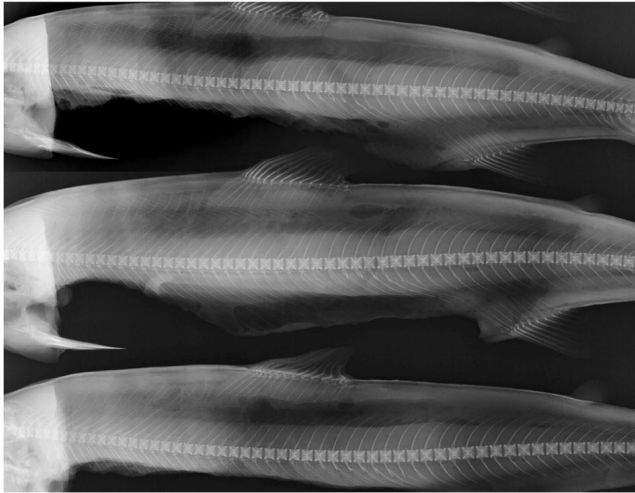
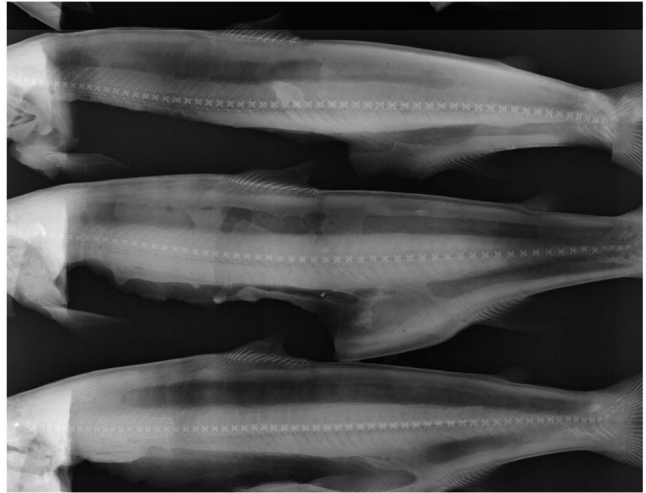
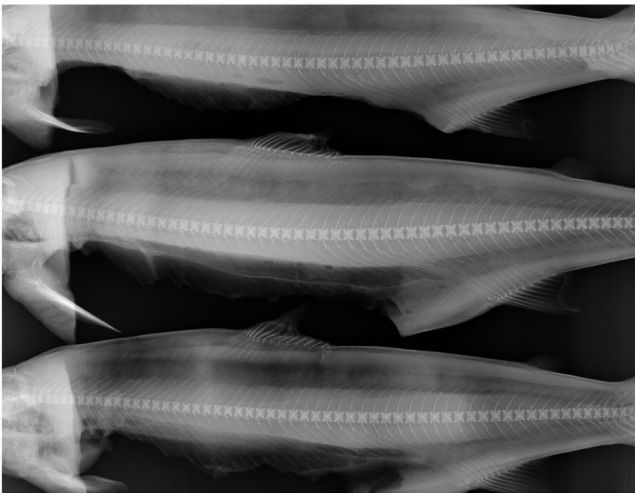
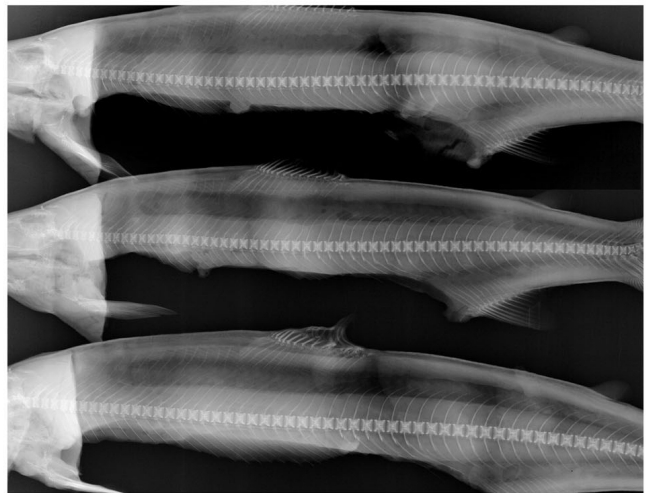
Vertebral bodies were analyzed for ash, Ca and P. For mineral analysis, soft tissue was removed and the bones were cleaned with demineralized water. Lipids were removed from the samples by rinsing the samples twice in a mixture of acetone and methanol (1:1, v/v). The samples were dried for 24 h at 105°C, ashed at 550°C for 18 h and digested according to the AOAC method (AOAC, 1995). The calcium and phosphorus content was determined colorimetrically (Taussky and Shorr, 1953). The analysis was carried out at Masterlab Analytical Services, Nutreco, Holland ([www.masterlab.nl](http://www.masterlab.nl)).

## RESULTS

### The P-deficient phenotype: no compression, no fusion

After 7 weeks of dietary P deficiency, the average mass of LP animals was 15% lower compared with control group animals (Table S2). After 16 weeks of P restriction, the mass difference increased to 20%. No significant differences were observed at any time for the condition factor (*K*). LP and LP-LP fed animals were smaller than control group (RP) animals, but with a normal body conformation (Table S2). Whole-body ash content and Ca and P values of vertebral bodies decreased significantly in LP animals to approximately 40% compared with RP animals after 7 weeks of P restriction. After additional 9 weeks of P restriction, whole-body ash, Ca and P values in LP-LP animals further decreased to less than one-third compared with RP-RP animals, as well as compared with LP-RP and LP-HP animals (Fig. 2B–E).

Examination of the radiographs indicated that, like in RP and RP-RP animals (Fig. 3A,C), the size and shape of vertebral bodies was uniform in LP and LP-LP animals (Fig. 3B,D). No malformations were diagnosed other than an apparent reduced vertebral body size. No spine bending (kyphosis, lordosis, scoliosis), no vertebral body compression and no fusions were recorded in the sampled animals, and no externally visible deformities were observed in any of the animals in the experiment. Compared with animals of the control group (Fig. 4A,C), intervertebral spaces appeared enlarged in LP animals (Fig. 4B) and further enlarged in LP-LP animals (Fig. 4D). The mineralized (radio-dense) part of vertebral bodies was reduced (Fig. 5A) but remained square (Fig. 5B). The radiograph-based diagnosis of reduced vertebral body size and enlarged intervertebral spaces was extended by whole-mount staining and by histological examinations. Whole-mount staining showed regularly shaped non-mineralized bone, not visible on radiographs (Fig. 6A). Likewise, sagittal sections showed the presence of vertebral body endplates and spongy bone (see Fig. 1 for definitions) in LP-LP animals, comparable to the extent of vertebral body endplates and spongy bone in RP-RP animals (compare Fig. 7A and B). Elongated osteoblasts (see Fig. 1 for the cells' location), typical of fast-growing salmon bone (Witten and Hall, 2002), were present in the vertebral body growth zone of LP-LP animals, as in animals from all diet groups (Fig. 7E–H). Likewise, the organization of intervertebral spaces and intervertebral ligaments remained unaltered. In summary, the LP diets did not induce vertebral column malformations, although X-rays show small and widely spaced vertebral bodies. Whole-mount staining and histological analysis revealed this as an X-ray artefact. Bone formation continued, and new bone had a regular structure, albeit without minerals.

**A** RP 7 weeks**B** LP 7 weeks**C** RP-RP 16 weeks**D** LP-LP 16 weeks**E** LP-RP 16 weeks**F** LP-HP 16 weeks

5 cm

**Fig. 3. Typical X-rays of Atlantic salmon from all six experimental groups.** (A) RP 7 weeks; (B) LP 7 weeks; (C) RP-RP 16 weeks; (D) LP-LP 16 weeks; (E) LP-RP 16 weeks; (F) LP-HP 16 weeks. The phenotype of fish within each group was homogeneous. Spines from animals in the LP and LP-LP groups (B,D) display reduced radiodensity. Note that all animals have straight spines without malformations such as fusion or compression. All figures are at the same magnification (see scale bar below F).

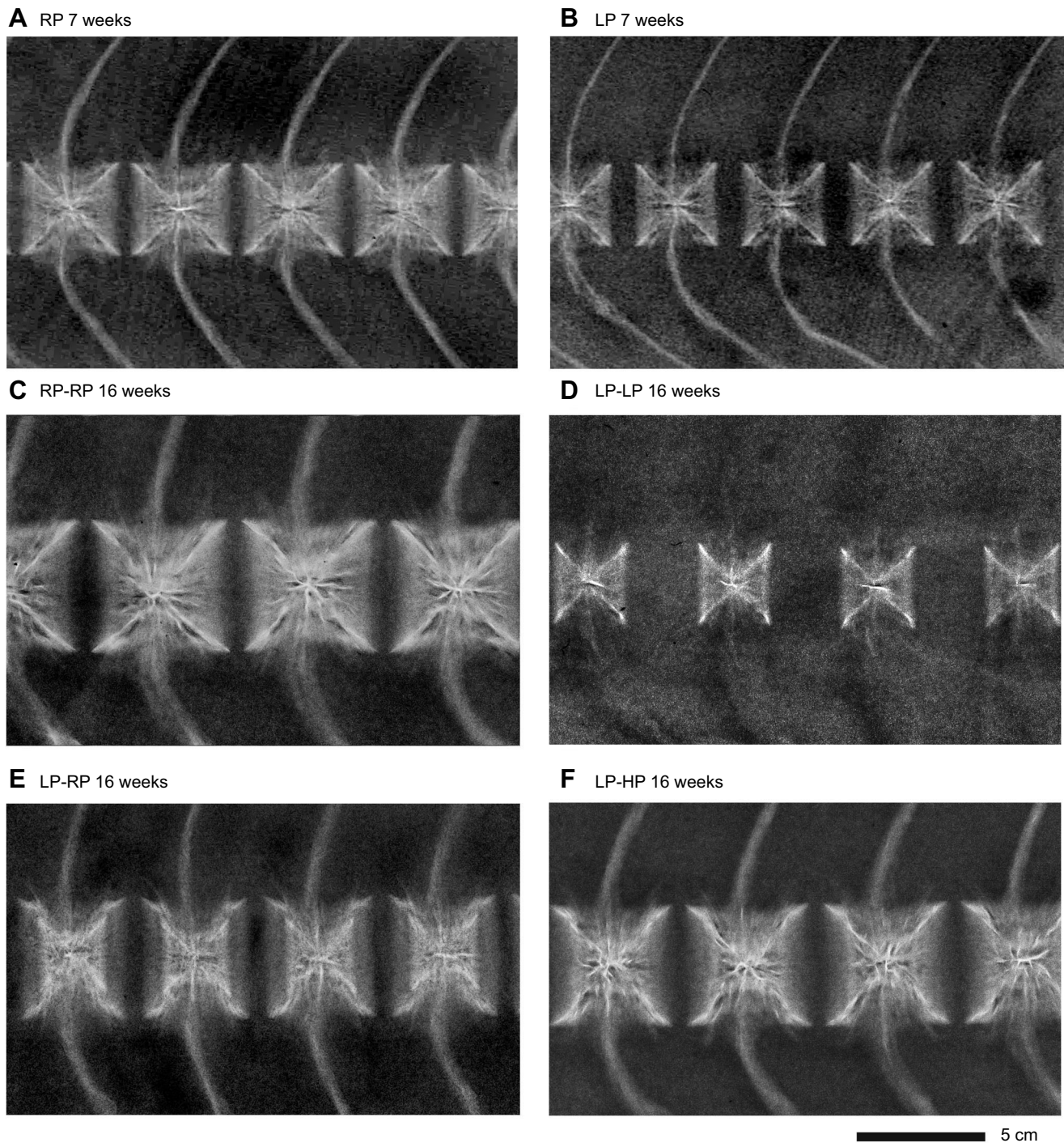


**Fig. 4. X-rays showing vertebral body details from Atlantic salmon from all six experimental groups.** (A) RP 7 weeks; (B) LP 7 weeks; (C) RP-RP 16 weeks; (D) LP-LP 16 weeks; (E) LP-RP 16 weeks; (F) LP-HP 16 weeks. Vertebral bodies from LP and LP-LP animals (B,D) appear small and widely spaced. In LP-RP animals (E) re-mineralization is underway and slightly further progressed in LP-HP animals (F). All figures are at the same magnification (see scale bar below F).

#### **Skeletal tissue alterations in P-deficient animals**

The most prominent tissue alteration in LP and LP-LP animals was the development of large amounts of non-mineralized bone (Figs 6A,C,D, 7J). In comparison, RP and RP-RP animals only had a narrow zone of non-mineralized bone, i.e. regular osteoid (Figs 6B,E, 7I). The arrest of bone matrix mineralization in LP and LP-LP animals is abrupt; a transitional zone of low mineralized bone was not observed. LP-LP animals develop ectopic cartilage in

the spongy bone region underneath the vertebral body endplates (Fig. 7M–O). This ectopic cartilage also occurs in LP-RP and LP-HP animals (see below), but was not observed in RP and RP-RP animals, or in LP animals.

#### **Reduced stiffness in P-deficient vertebrae can be restored**

LP-LP vertebrae show a high amount of deformation, which separated this group clearly from all other groups. At 40 N load, the

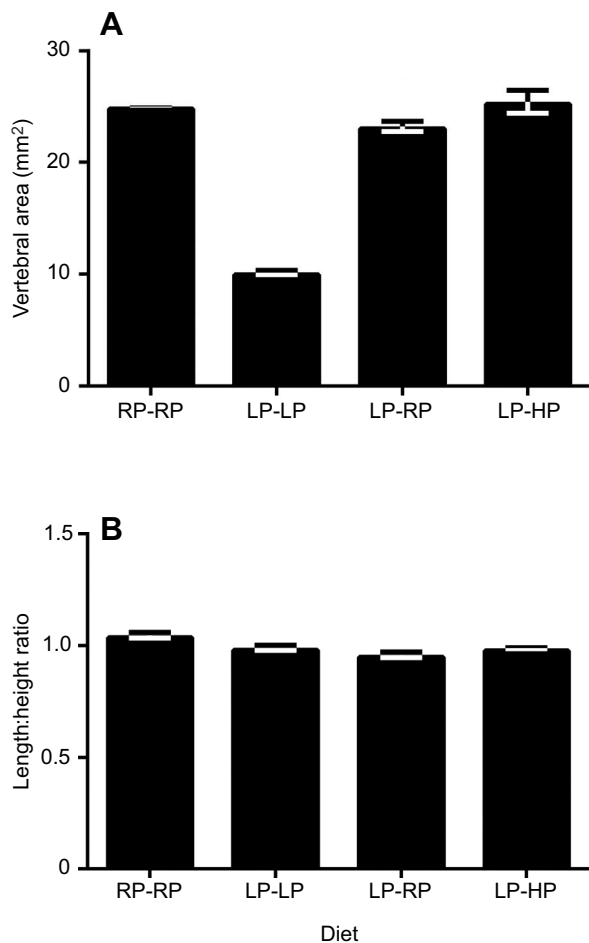


**Fig. 5. Measurements of vertebral body size based on X-rays.** Vertebral centrum area (A) and length/height ratio (B) of vertebral bodies as measured on X-rays at the end of the experiment. No significant differences concerning size and shape are detected between vertebral bodies from the RP-RP, LP-RP and LP-HP groups. The radio-dense, mineralized part of vertebral bodies from the LP-LP group is significantly reduced (A) without concomitant alterations of the length to height relationship (B). Bars on top of each column indicate  $\pm$ s.d.

reduction in cranial–caudal length (i.e. deformation) of the LP-LP vertebrae was approximately five times higher than in the LP-RP, LP-HP and RP-RP vertebrae (Fig. 8). The stiffness of the vertebrae was significantly lower in LP-LP vertebrae compared with all other groups, and significantly lower in the LP-RP vertebrae compared with the LP-HP and RP-RP vertebrae (Table S3).

### Bone is capable of secondary mineralization in P-deficient salmon

After 7 weeks of P-deficient diet and the development of large amounts of non-mineralized bone, the diet in four tanks with LP-fed animals was changed to RP or to HP for another 9 weeks (Fig. 2A) to determine whether non-mineralized bone could still mineralize. In animals from both groups (LP-RP and LP-HP), values for ash, Ca and P largely recovered (Fig. 3B,D,E). The P values in LP-RP and LP-HP did not show significant differences compared with those of RP-RP animals. All measured values remained significantly different between the animals from the LP-LP group compared with all other groups (Fig. 2B–E). X-rays of LP-RP and LP-HP animals show vertebral bodies that regained radiodensity with no

signs of significant compression (Figs 3E,F, 4E,F). Detailed radiograph scans show almost complete re-mineralization in LP-HP animals (Fig. 4F). This was confirmed by the histological analysis. The zone of non-mineralized bone in LP-HP animals narrowed to a size similar to that in RP-RP animals (Fig. 7I,L). In LP-RP animals, non-mineralized bone also mineralized, but the zone of non-mineralized bone was slightly broader than in LP-HP animals (Fig. 7K,L). Secondary mineralization in LP-RP and LP-HP animals was always continuous with the last mineralized part located deep inside the bone.

### Traces of a P-deficiency history

Secondary mineralization progressed homogeneously in all parts of the vertebral bodies, i.e. in the bone trabeculae and in the vertebral body endplates, albeit with one exception. In the vertebral body endplates, a ring-shaped zone remained lowly or non-mineralized in LP-RP and LP-HP animals (Fig. 9A,B). This zone explains areas of reduced radiodensity that can be identified on X-rays of LP-RP and LP-HP animals (Fig. 9C). Histological sections showed this zone and its co-localization with ectopic cartilage that develops proximal to the vertebral body endplate (Fig. 9D–F). The ectopic cartilage was also observed in LP-LP animals (Fig. 7M–O). Different from LP-LP animals, the ectopic cartilage in LP-RP and LP-HP animals had started to mineralize (Fig. 9F) and was obviously resorbed together with the adjacent bone tissue (Fig. 9G). This indicates that the ectopic cartilage is not permanent and will eventually disappear in the course of re-mineralization and bone remodeling.

### Intervertebral ligaments remain intact under P-deficient conditions

The most common types of vertebral body deformities, compression and fusion, are characterized by alterations of the intervertebral ligaments and the notochord tissue in the intervertebral space (Witten et al., 2005, 2006; Ytteborg et al., 2010). None of the groups in this study displayed signs of structural alterations of intervertebral ligaments or of the notochord tissue in the intervertebral space (Figs 7A–D, 9H,I). Alterations that would foreshadow vertebral body compression or fusion were not recorded. The ligament that connects the edges of adjacent vertebral body endplates consists (from inside to outside, see also Fig. 1) of a thin elastin layer, the thickened notochord sheath, an outer elastin layer and type 1 collagen fiber bundles that connect the bone of the endplates and continue inside the bone as Sharpey fibers (Fig. 9H,I). All components of the ligament were present, well developed and unaltered in animals of all groups, including the LP-LP animals.

## DISCUSSION

### The primary bone pathology of dietary P deficiency

Teleost fish compensate for a shortage of dietary Ca by Ca intake via the gills, but depend on dietary P intake (Vielma and Lall, 1998). Thus, dietary P deficiency is widely assumed to cause skeletal malformations in farmed salmon (Baeverfjord et al., 1998; Sullivan et al., 2007a,b; Fjellidal et al., 2009, 2012a). Sufficient dietary P supply is required for fast-growing Atlantic salmon at all life stages (Fjellidal et al., 2012b; Smedley et al., 2018), and triploid Atlantic salmon have been reported to have an increased P demand (Fjellidal et al., 2016).

Given the long period of severe P deficiency in LP-LP animals, the development of pronounced osteomalacia was expected, but the absence of other severe bone pathologies was surprising. This warrants a discussion about the connection between dietary P deficiency and malformations commonly associated with P

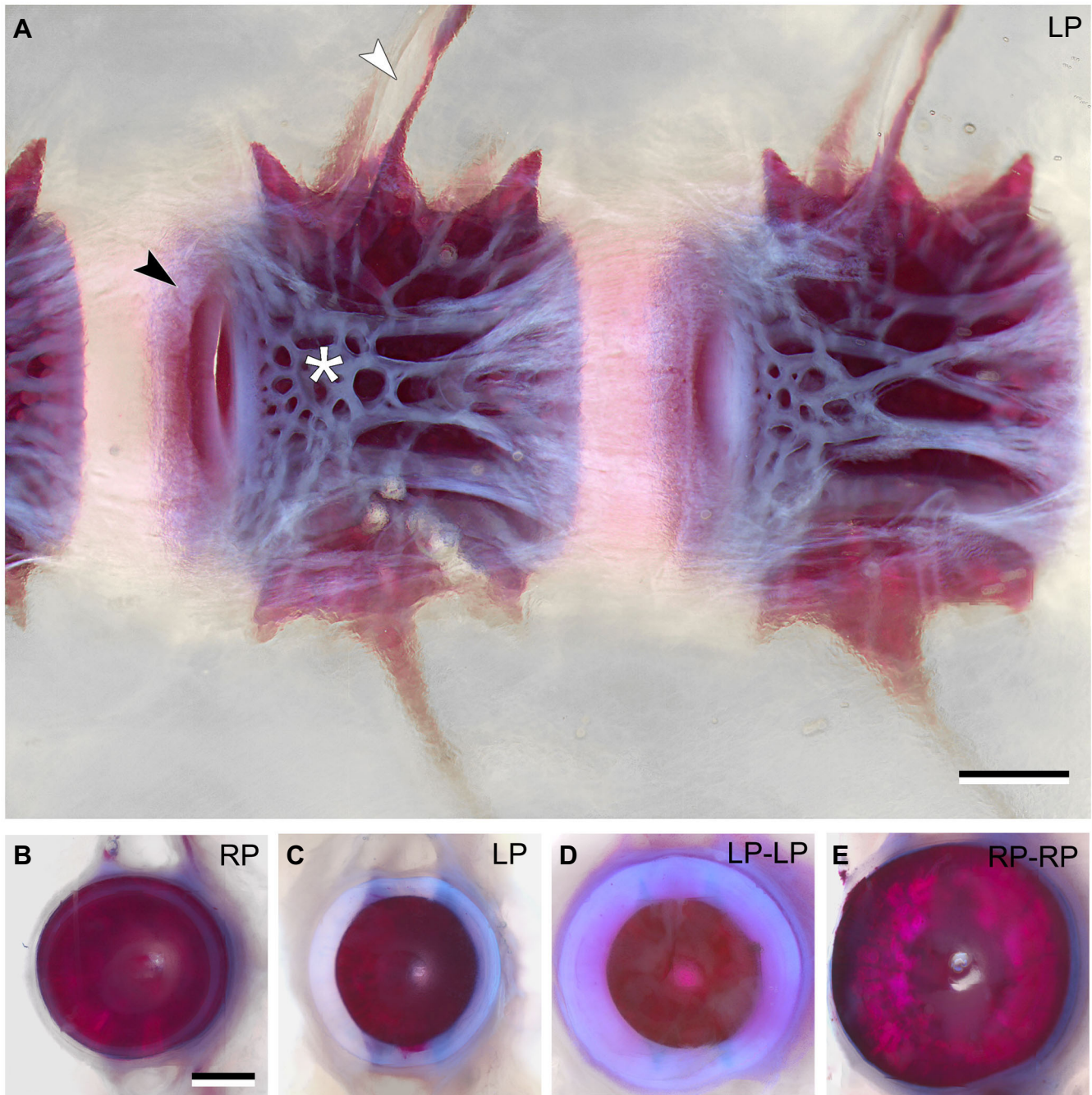


**Fig. 6. Mineralized and non-mineralized bone of vertebral bodies, whole-mount stained with Alizarin Red S, after 7 weeks and after 16 weeks.** (A) In an LP animal, non-mineralized bone (white) extends from the mineralized bone core (red). The white asterisk indicates non-mineralized spongy bone trabeculae. The black arrowhead indicates the non-mineralized part of the vertebral body endplate. Also, neural arches continue to add non-mineralized bone (white arrowhead). Scale bar: 1 mm. (B–E) Axial view of vertebral body endplates, indicated in A with a black arrowhead. (B) RP, (C) LP, (D) LP-LP and (E) RP-RP animals. Vertebral endplates (red) in LP (C) and LP-LP (D) animals continue to grow, albeit the bone matrix is completely void of minerals (white). A distinct border between mineralized and non-mineralized bone is visible. Size and structure of endplates with non-mineralized bone (C,D) are similar to mineralized endplates. B–E are at the same magnification, scale bar in B: 1 mm.

deficiency (Baeverfjord et al., 2012, 2018). After exposing animals to 7 and then 16 weeks of P deficiency, one would expect to find tissue alterations that foreshadow the development of vertebral body compression and fusion. Vertebral body compression is characterized by the appearance of ectopic fibrocartilage in the intervertebral space, fibrocartilage that replaces the intervertebral ligaments, the notochord tissue, and the osteoblasts of the vertebral

body growth zone (Kvallestad et al., 2000; Witten et al., 2005, 2009; Ytteborg et al., 2010). The ectopic cartilage restricts the elongation of vertebral bodies and facilitates only the increase in diameter. This leads to the compression phenotype (Witten et al., 2005). Subsequently, mineralization of the fibrocartilage can trigger its remodeling into bone with the consequence of complete vertebral body fusion (Witten et al., 2006). In the current study, no ectopic



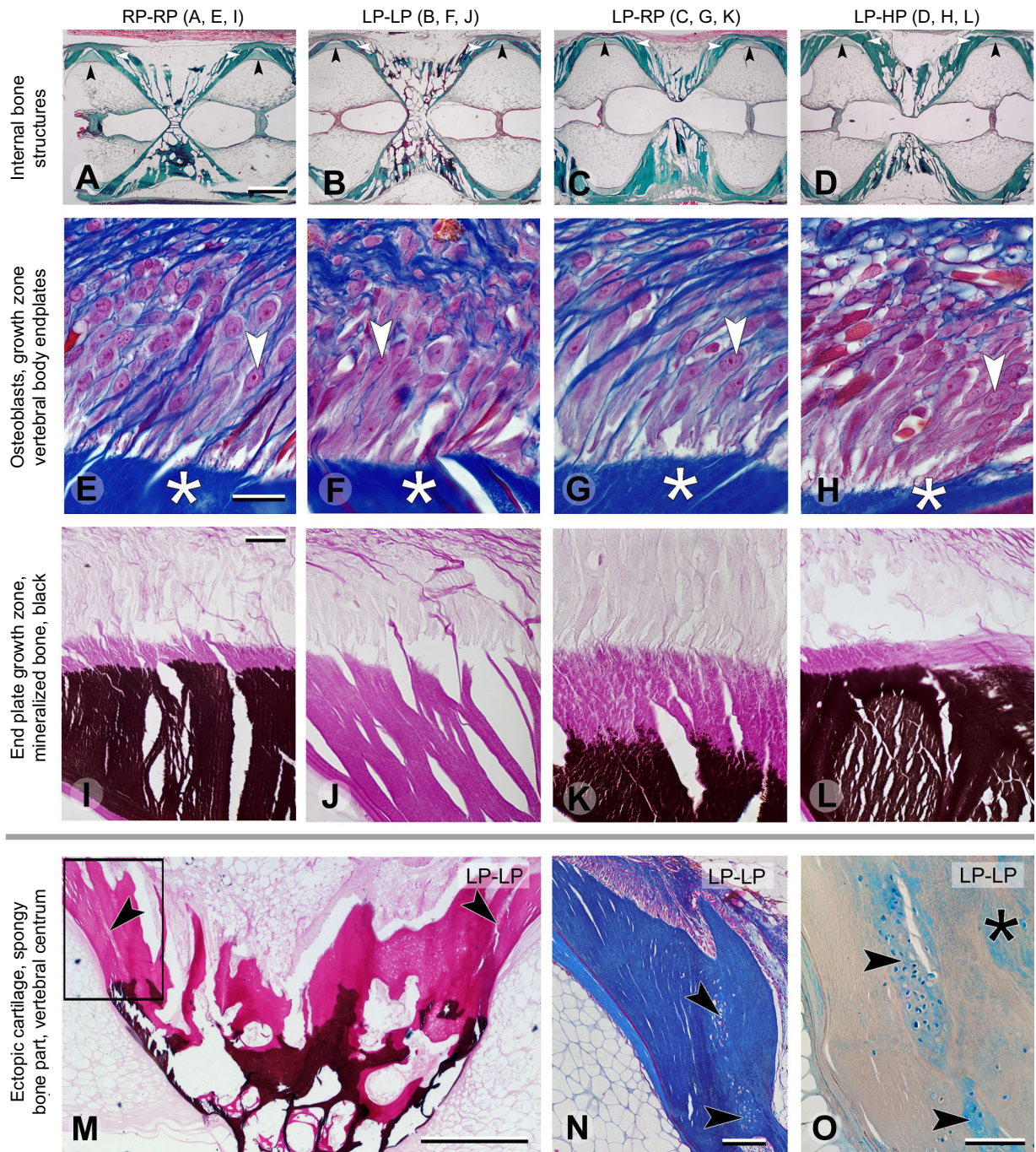


**Fig. 7. Sagittal sections close to the midline of the vertebral column showing the extent of mineralized and non-mineralized bone, osteoblasts, patterns of secondary mineralization and ectopic cartilage.** (A–D) One vertebral body and two adjoining intervertebral spaces, sampled at the end of the experiment. (A) RP-RP, (B) LP-LP, (C) LP-RP and (D) LP-HP groups. Vertebral body endplates are fully extended in all groups. Intervertebral ligaments are present in the intervertebral space and unaltered (see also Fig. 10H,I). See boxed gray area in Fig. 1 for the location. Black arrowheads, intervertebral spaces with thickened notochord sheath. White arrowheads, vertebral body endplates. Masson's trichrome staining; A–D are at the same scale, scale bar in A: 500  $\mu$ m. (E–H) Osteoblasts in the growth zone of vertebral body endplates (see Fig. 1 for osteoblast location). Assignment to groups as for A–D. White asterisks indicate the osteoid; white arrowheads indicate osteoblasts. Osteoblasts in all groups are elongated and located between Sharpey fibers. There is no histological indication for a reduced osteoblast activity in LP-LP animals (F) or enhanced osteoblast activity in LP-HP animals (H). Azan staining; E–H are at the same magnification, scale bar in E: 20  $\mu$ m. (I–L) Status of bone mineralization and secondary mineralization in the growth zone of vertebral body endplates (see Fig. 1 for the vertebral body endplate growth zone). Assignment of groups as for A–D. Mineralized bone, black; non-mineralized bone (collagen), red. The bone in LP-LP animals remains non-mineralized (J). Secondary mineralization in LP-RP animals is well underway (K). Secondary mineralization appears complete in LP-HP animals (L). Von Kossa staining; I–L are at the same magnification, scale bar in I: 50  $\mu$ m. (M) Sagittal section, upper half of an LP-LP vertebral body (see upper half of boxed gray area in Fig. 1), staining as in I–L. Large amounts of non-mineralized bone are present after 16 weeks of P-deficient diet. The black arrowheads indicate the location of ectopic cartilage that has developed, shown in more detail in N and O. Scale bar: 500  $\mu$ m. (N) LP-LP animal. Higher magnification of ectopic cartilage (black arrowheads; location, see box in N) that developed underneath the vertebral body endplates. Azan staining, scale bar: 100  $\mu$ m. (O) LP-LP animal. The matrix of the ectopic cartilage stains positive for Alcian Blue (black arrowheads). There is also increased Alcian Blue staining in areas of non-mineralized spongy bone (black asterisk). Alcian Blue/Hematoxylin staining, scale bar: 50  $\mu$ m.

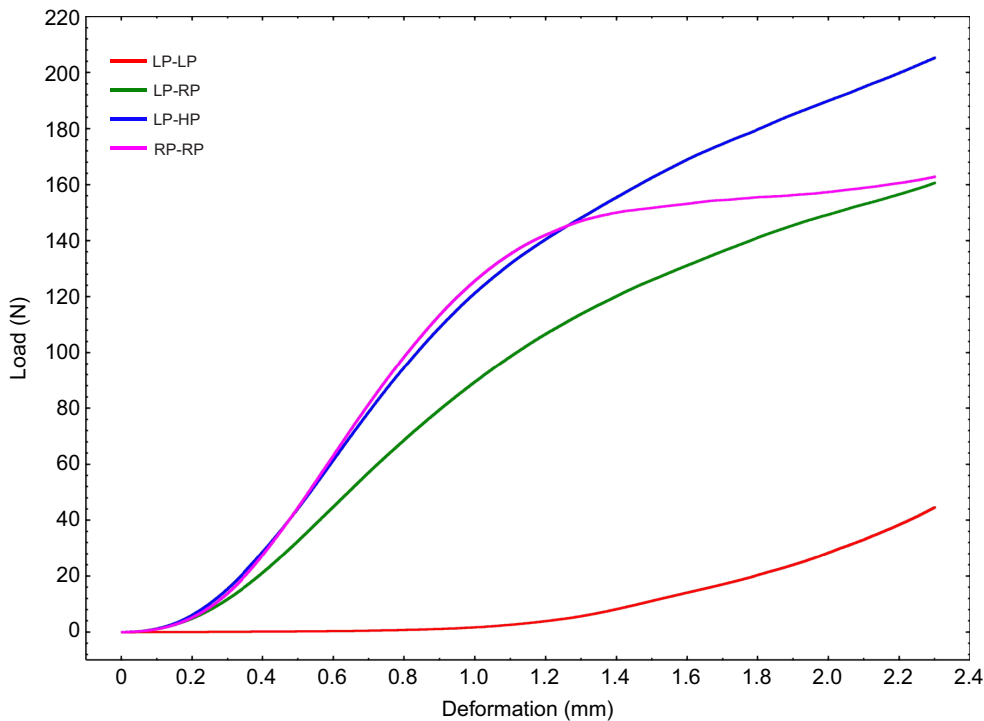


**Fig. 8. Deformation data of vertebral bodies.** The graph shows the relationship between the deformation in millimeters (x-axis) and the load in Newtons (y-axis). The lines represent the mean values for each dietary group.

cartilage in the intervertebral space was observed. Moreover, no tissue alterations in the intervertebral space or alterations in the vertebral body growth zone were observed. This strongly suggests that P deficiency as a single factor is not causative for vertebral body compression and fusion, at least not in the life stage studied.

Although no alterations of tissues in the intervertebral space were detected (Fig. 9H,I), ectopic cartilage located proximal to the vertebral body endplates had developed in LP-LP, LP-RP and LP-HP animals at the end of the experiment (Figs 7M–O, 9E–G). The ectopic cartilage was located in the spongy bone part of the vertebral centrum (see Fig. 8N). According to Laerm (1976), this spongy bone is formed in response to mechanical load. The development of cartilage in this region can thus be explained by the influence of biophysical stimuli. Strain induces the development of fibers (and subsequently bone) whereas compression induces the formation of cartilage (Pauwels, 1960; Weinans and Prendergast, 1996; Boccaccio and Pappalettere, 2011). With functional intervertebral spaces and non-mineralized (soft) vertebral body endplates, compressive load from the vertebral body joints was likely transmitted to the non-mineralized spongy bone. This compression would then have triggered the development of ectopic cartilage. The history of this compression is reflected by slight shape alterations of vertebral bodies from LP-RP and LP-HP animals (Fig. 10A–D). Vertebral body endplates during the phase of P deficiency appear slightly bent inwards. Subsequently, and likely related to re-feeding with sufficient P, the endplates resume a regular angle. Similar shape alterations have been observed by Fjellidal et al. (2007) in Atlantic salmon, with low mineralized vertebral bodies 12 weeks after seawater transfer. The fact that a ring-shaped zone of soft, non-mineralized bone adjacent to the ectopic cartilage remains in LP-RP and LP-LP animals (Fig. 9A,B) can explain the persistence of this cartilage. The ectopic cartilage is located in a region of the vertebral body where remodeling is common. Accordingly, resorption of mineralized ectopic cartilage was observed (Fig. 9G). It can thus be expected that the cartilage will

eventually remodel into bone and disappear again. This is different from ectopic cartilage that develops in the intervertebral space. This cartilage is lasting, and mineralization and remodeling of this cartilage into bone cause vertebral body fusion (Witten et al., 2005, 2006).

#### Mineralization of P-deficient non-mineralized bone

Research that uses zebrafish (*Danio rerio*) as a model to study human bone diseases often does not distinguish between bone formation and mineralization given that only bone mineral density is measured. However, bone formation and bone mineralization are not the same. Techniques to visualize the extreme small bone elements in early zebrafish, Alizarin Red S whole-mount staining and micro CT, suffer from the same drawback as X-rays. Without oblique illumination (whole-mount staining) or contrasting agents (micro CT, X-rays) these techniques show only the mineralized phase of the bone (Bruneel and Witten, 2015; Witten et al., 2017). The fact is that during early bone formation in zebrafish, mineralization starts only 5 to 6 h after osteoid deposition (Cubbage and Mabee, 1996; Bird and Mabee, 2003). We are not aware of such data for teleost species that have larger individuals, for example, Atlantic salmon. In human bone, the delay of osteoid mineralization is the norm. Osteoid mineralization may start as late as 10 days after bone matrix formation (Boivin and Meunier, 2002). Although the 7-week mineralization delay that was enforced in this experiment is a much longer period, the principle appears to be the same. In the context of normal bone formation, bone matrix is produced first and mineralization happens later. Similar to the current findings, it is also possible to re-mineralize non-mineralized human bone matrix in the case of P-deficiency-related osteomalacia (Allen and Raut, 2004; Wilton et al., 1987). This and the findings of the present study underscore the distinction between bone formation and mineralization (Kyle, 1927; Beresford, 1981). The pattern of secondary mineralization raises questions about the role of osteoblasts in this process. If mineral deposition directly depends on osteoblasts, secondary mineralization in salmon should start in

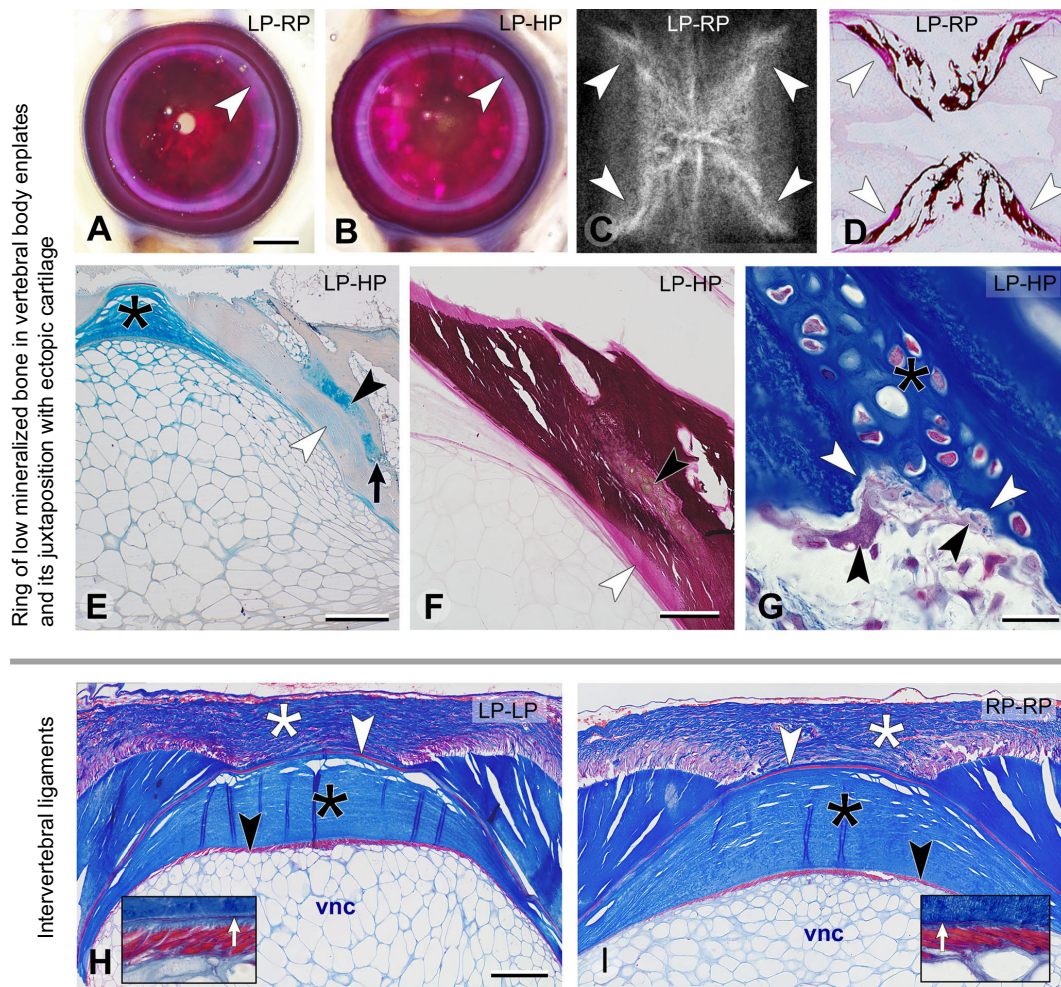


**Fig. 9. A ring of low mineralized bone in the vertebral body endplates of LP-RP and LP-HP group animals and intact intervertebral ligaments.**

(A,B) Alizarin Red S whole-mount staining. Axial view on vertebral body endplates from LP-RP and LP-HP animals that underwent secondary mineralization. In both groups, a ring-shaped zone of non-mineralized bone persists (white arrowheads). (C) The ring-shaped zone of non-mineralized bone shown in A and B can be aligned with radio-translucent areas visible on X-rays at higher magnification (white arrowheads). (D) The non-mineralized ring (red) is also visible (white arrowheads) on sagittal histological sections stained for minerals (black) with the Von Kossa/Van Gieson protocol. A–D are at the same magnification, scale bar in A: 1 mm. (E) Residues of ectopic cartilage in an LP-HP animal. The cartilage (black arrowhead) is located next to the ring of low mineralized bone in the vertebral endplate (white arrowhead). The ring of low mineralized bone stains stronger with Alcian Blue than the mineralized bone. The notochord sheath (black asterisk) stains like cartilage matrix. The black arrow indicates the site of bone and cartilage resorption, shown in G. Alcian Blue/Hematoxylin staining, scale bar: 300  $\mu$ m. (F) Mineralization of the ectopic cartilage (black arrowhead) in an LP-HP group animal. Same location as E. The white arrowhead indicates the ring of non-mineralized bone. Von Kossa/Van Gieson staining, scale bar: 100  $\mu$ m. (G) LP-HP group animal. Resorption of bone and ectopic cartilage, see black arrow in E. Black arrowheads indicate osteoclasts and chondroclasts with typical ruffled borders. White arrowheads indicate resorption lacunae and areas of cartilage degradation. Resorption of the mineralized cartilage (see F) suggests that this cartilage is not permanent and will disappear in the frame of remodeling. Azan staining, scale bar: 20  $\mu$ m. (H,I) Intervertebral spaces of LP-LP and RP-RP animals, respectively. Intervertebral ligaments show a regular structure consisting of the notochord sheath (black asterisks), the outer elastin layer (white arrowheads) and collagen fiber bundles that connect the edges of the vertebral body endplates (white asterisks). Vacuolated notochord cells (vnc) and the cells of the notochord epithelium (black arrowheads) are intact. The insets show the cells of the notochord epithelium at higher magnification. Also visible is the thin inner elastin layer (white arrows). Azan staining; H and I are at the same magnification, scale bar in H: 100  $\mu$ m, insets: 20  $\mu$ m.

the cells' vicinity. This would generate a zone of mineralized bone adjacent to the osteoblasts on top of deeper located non-mineralized bone. In the present study, however, there was no indication for such a pattern (Fig. 10G, compare with 10E,F). Mineralization of the bone matrix was always continuous with the last mineralized part of the bone (Fig. 10F). Re-mineralization started far away from the osteoblasts, suggesting that, at this point, osteoblasts are not actively involved in mineralization. This would be in line with Hamlin and Price (2004), who concluded that mineralization of bone matrix requires serum but not cells.

Studies on human bone show that mineralization is a biphasic process. The primary phase of mineralization (about 50%) is rapid

whereas completion of mineralization is slow and can last for months or years (Boivin and Meunier, 2002). The steep slope at the beginning of mineralization and the significant reduction in the slope later is also referred to as the mineralization law. The strength of bone quickly increases during the primary phase of mineralization. Even a small elevation of the mineral content can have a large effect (Neel et al., 2016). This may explain why similar load–strain curves were observed in RP-RP, LP-RP and LP-HP animals, curves that were distinctively different from the load–strain curves of LP-LP animals (Fig. 8). The reduction of the osteoid zone in LP-HP animals (Fig. 7M) and the restoration of calcium and phosphate levels (Fig. 2D,E) indicate rapid re-mineralization in

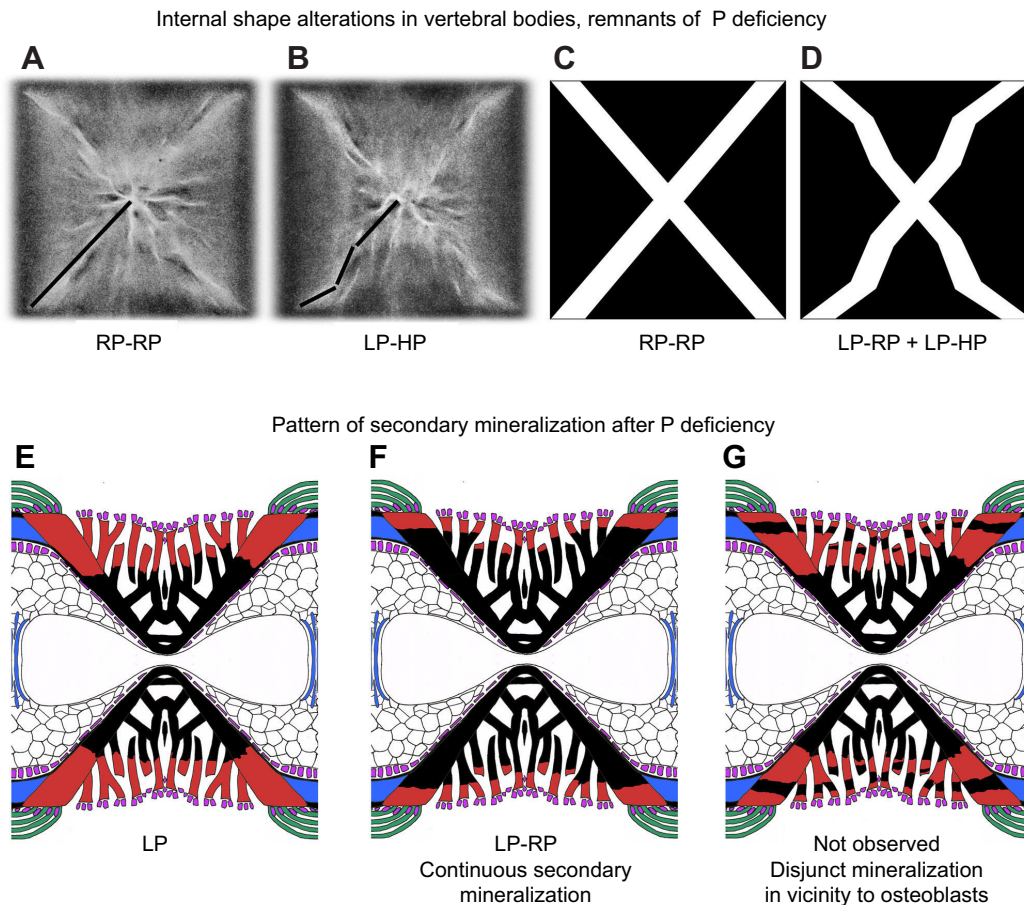


**Fig. 10. Internal structure and mineralization pattern in vertebrae of P-deficient animals.** (A–D) Internal shape alterations and pattern of secondary mineralization of vertebral bodies from LP-RP and LP-HP group animals that restored their mineral content. On X-rays, vertebral body endplates in RP-RP animals form a straight X, indicated by the black line in A and by the cartoon in C. (B) In LP-HP (as well as in LP-RP) group animals, the period of P deficiency likely causes slight inward bending of the vertebral body endplates, whereas bone that forms during P restoration bends again outwards, indicated by the black line in B and by the cartoon in D. (E,F) The cartoons show the pattern of secondary mineralization after the period of P deficiency. Mineralization is always continuous, and a situation as shown in G is therefore not observed. Secondary mineralization starts deep inside the bone matrix and not in the vicinity of osteoblasts. Mineralized bone is indicated in black, non-mineralized bone in red; for other structures, see labels in Fig. 1.

LP-HP animals. One can speculate that re-mineralization is essentially complete and only the rearrangement of the mineral crystals needs to be accomplished (Barragan-Adjemian et al., 2006). In LP-RP animals, re-mineralization appears to be slightly less complete, principally indicated by the broader osteoid seam at the end of the experiment (Fig. 7I). Mineral analysis, shape of the vertebrae and the load–strain curves show a trend but no significant differences, indicating that in the LP-RP group re-mineralization is also well underway.

#### Failure to generate main skeletal pathologies with a P-deficient diet

For different reasons, it is desirable to restrict the amount of P in fish feeds. First, the protection of marine fish stocks requires the replacement of fish meal as a source of P in salmon feeds. Second, P-containing effluents from fish farms are regarded as pollutants. Third, P resources are limited and the growing aquaculture sector competes with agriculture for inorganic P. Because dietary P cannot be limited for reasons of animal health and welfare, it is desirable to determine which pathologies are caused by low-P diets or whether even fish health-related reasons exist to restrict the dietary P content (Sugiura et al., 2004; Naylor et al., 2009; Cordell et al., 2011).

P deficiency in freshwater stages of Atlantic salmon causes skeletal malformations, but the exact nature of the pathological alterations on the microstructure of bone and cartilage still need to be determined (Smedley et al., 2018). The current study with early seawater stages failed to generate any skeletal pathology that would lead to vertebral body fusion or compression after 16 weeks of feeding with a low P diet. We currently do not know whether this would be also the case in freshwater stages. Other skeletal pathologies that have been associated with P deficiency in Atlantic salmon were also not generated in the present study (Fjelldal et al., 2014; Amoroso, 2016; Baevefjord et al., 2018). No increased bone resorption, no microfractures, no curling of ribs, no mouth gaping and no ectopic fibrous tissue in the musculature were detected. Moreover, it was possible to restore the mineral content of the bone after 7 weeks of severe P deficiency. This strongly suggests that much less severe and shorter-term P deficiencies that may occur under farming conditions cannot be the single or primary cause for skeletal malformations, at least not in the animals' seawater phase. No deformities were produced after feeding salmon an LP diet for 16 weeks in seawater tanks at 12°C under continuous light. In contrast, Fjelldal et al. (2012c) found a reduced vertebra length/dorso-ventral diameter, indicating an ongoing deformity

development, after feeding salmon a low P diet at 16°C in seawater tanks under continuous light for 11 weeks. This effect was not seen under a 12 h:12 h light:dark cycle in the same study (Fjelldal et al., 2012c). The present study and the Fjelldal et al. (2012c) experiments were both performed in tanks with stable environmental conditions, whereas sea cage aquaculture, with a much more unstable environment, is the main production technique for farming salmon in seawater. Studying how dietary P level affected mineralization and development of vertebra deformities in salmon in sea cages, Fjelldal et al. (2009) fed salmon post-molts two dietary levels of P for 17 weeks, and followed the fish up to harvest size. In that study, radiological deformities were produced in fish fed the lowest dietary P content already after 17 weeks. In the current experiment, under stable and controlled tank conditions, P deficiency as a single factor has no consequences other than growth reduction. It thus becomes important to search for co-factors or even other primary factors that might have triggered the development of vertebral column malformations. Gil-Martens et al. (2012) tested, and rejected, the hypothesis that dietary P deficiency and inflammation are co-factors for vertebral body malformations.

### Can bone function without minerals?

If non-mineralized bone can be mineralized later or stay non-mineralized without lasting consequences, the question remains as to why severe osteomalacia did not cause severe bone disorders. A possible explanation relates to the environment in which the fish skeleton functions. Water imposes a different type of stress on the vertebral column of teleosts compared with land-dwelling amniotes. The swim bladder mitigates the effects of gravity, and the application of force in movement on the joints of the axial skeleton is muscle related (Witten and Huysseune, 2009; Longo et al., 2013). Teleost fish only use about 10% of their axial musculature (slow-twitch red muscle fibers) for continuous swimming. Ninety percent of the axial muscles (fast-twitch white muscle fibers) are only used for acceleration in the dense medium (compared with air), water (Johnston, 1981; Rome, 2000). Under stable and controlled tank conditions, the fast-twitch white muscle fibers are likely not used and non-mineralized bone is apparently strong enough to sustain regular swimming. Moreover, a straight correlation between the degree of bone mineralization and bone quality does not exist. The toughest known vertebrate bones are deer antlers, characterized by their low mineral content (Currey, 1999, 2003). In human infants, low mineralized bone will bend but will not fracture. Likewise, not osteomalacia but over-mineralization increases the risk for fractures and microfractures in human bone (Wilton et al., 1987; Guglielmi et al., 2011). While the collagenous matrix provides toughness (fracture resistance), the minerals increase the bones' stiffness (bending resistance) (Viguet-Carrin et al., 2006). The mineral phase alone is brittle and bone strength largely depends on the non-mineralized matrix: type 1 collagen fibers arranged according to the direction of mechanical load. Indeed, collagenous bone matrix without minerals can be tougher than mineralized bone (Currey, 2003; Viguet-Carrin et al., 2006). This can perhaps add an explanation to the question of why advanced teleost species from orders that live in the deep sea or at high latitudes (e.g. Gadiformes, Perciformes, Ophidiiformes, Scorpaeniformes, Stomiiformes) can afford to have extremely low mineralized skeletons (Günther, 1878; Denton and Marshall, 1958; Phleger, 1988). Another non-mineralized structure that can support the axial skeleton is the notochord. Although most actinopterygians and tetrapods have mineralized vertebral bodies, the fossil record of

actinopterygians provides ample examples that the axial skeleton functions without mineralized vertebral bodies. Instead, the notochord has been the main axial support (Maisey, 1991, 2000). The vertebral column of large actinopterygians and sarcopterygian individuals such as sturgeons, coelacanths and lungfish is supported by an uninterrupted notochord as the functional axial skeleton. Mineralized vertebral bodies are lacking (Arratia et al., 2001). In the current experiment, the structure of the notochord located in the intervertebral spaces remained unaltered in animals from all groups. The functional notochord perhaps also explains why a functional vertebral column was maintained during periods of P deficiency.

### Acknowledgements

We thank Iselin Rusten and the staff of the Lerang Research Station for their help in conducting the feeding experiments, and Mieke Soenens from Ghent University for helping with the histological analysis. We thank Brian Eames and one anonymous reviewer for their very helpful comments on the manuscript. The Skretting Aquaculture Research Centre (Stavanger, Norway) provided the experimental diets and the salmon rearing facilities for the experiments.

### Competing interests

The authors declare no competing or financial interests.

### Author contributions

Conceptualization: P.E.W., A.H., C.M., A.O., M.A.G.O.; Methodology: P.E.W., P.G.F., A.H., A.O., M.A.G.O.; Software: P.G.F.; Validation: P.G.F., A.O., M.A.G.O.; Formal analysis: P.E.W., P.G.F., A.H., M.A.G.O.; Investigation: P.E.W., P.G.F., M.A.G.O.; Resources: A.H., C.M., A.O., M.A.G.O.; Data curation: P.E.W., P.G.F., M.A.G.O.; Writing - original draft: P.E.W.; Writing - review & editing: P.E.W., P.G.F., A.H., M.A.G.O.; Visualization: P.E.W.; Supervision: P.E.W., A.O., M.A.G.O.; Project administration: C.M., A.O., M.A.G.O.; Funding acquisition: C.M., A.O., M.A.G.O.

### Funding

This research received no specific grant from any funding agency in the public, commercial or not-for-profit sectors.

### Supplementary information

Supplementary information available online at <http://jeb.biologists.org/lookup/doi/10.1242/jeb.188763.supplemental>

### References

- Albrektsen, S., Hope, B. and Aksnes, A. (2009). Phosphorous (P) deficiency due to low P availability in fishmeal produced from blue whiting (*Micromesistius poutassou*) in feed for under-yearling Atlantic salmon (*Salmo salar*) smolt. *Aquaculture* **296**, 318-328.
- Allen, S. C. and Raut, S. (2004). Biochemical recovery time scales in elderly patients with osteomalacia. *J. Roy. Soc. Med.* **97**, 527-530.
- Amoroso, G. (2016). Investigations of skeletal anomalies in triploid Atlantic salmon (*Salmo salar* L. 1758) in freshwater with particular focus on lower jaw deformity (LJD). *PhD thesis*, Institute for Marine and Antarctic Studies, University of Tasmania, Launceston, Tasmania.
- Antonucci, R., Locci, C., Clemente, M. G., Chicconi, E. and Antonucci, L. (2018). Vitamin D deficiency in childhood: old lessons and current challenges. *J. Pediatr. Endocr. Met.* **31**, 247-260.
- AOAC (1995). *Official Methods of Analysis of AOAC International*, 16th edn. Arlington, VA: Association of Official Analytical Chemists.
- Arratia, G., Schultze, H. P. and Casciotta, J. (2001). Vertebral column and associated elements in dipnoans and comparison with other fishes: Development and homology. *J. Morphol.* **250**, 101-172.
- Baeverfjord, G., Åsgård, T. and Shearer, K. D. (1998). Development and detection of phosphorous deficiency in Atlantic salmon, *Salmo salar* L., parr and post-smolts. *Aquacult. Nutr.* **4**, 1-11.
- Baeverfjord, G., Fjelldal, P. G., Albrektsen, S., Hatlen, B., Denstadli, V., Ytteborg, E., Takle, H., Lock, E.-J., Berntssen, M. H. G., Lundebye, A. K. et al. (2012). *Mineral nutrition and the impact on bone development and skeletal deformities – a review*. Nofima Report 37/2012, 1-91, Tromsø, Norway: Nofima AS.
- Baeverfjord, G., Antony Jesu Prabhu, P., Fjelldal, P. G., Albrektsen, S., Hatlen, B., Denstadli, V., Ytteborg, E., Takle, H., Lock, E.-J., Berntssen, M. H. G. et al. (2018). Mineral nutrition and bone health in salmonids. *Rev. Aquacult.* 1-26.
- Barragan-Adjemian, C., Nicoletta, D., Dusevich, V., Dallas, M. R., Eick, J. D. and Bonewald, L. F. (2006). Mechanism by which MLO-A5 late osteoblasts/early osteocytes mineralize in culture: similarities with mineralization of lamellar bone. *Calc. Tiss. Int.* **79**, 340-353.

- Bensimon-Brito, A., Carreira, J., Cancela, M. L., Huysseune, A. and Witten, P. E. (2012). Distinct patterns of notochord mineralization in zebrafish coincide with the localization of Osteocalcin isoform 1 during early vertebral centra formation. *BMC Dev. Biol.* **12**, 28.
- Beresford, W. A. (1981). *Chondroid Bone, Secondary Cartilage and Metaplasia*. Baltimore-Munich, USA, Germany: Urban & Schwarzenberg.
- Berge, G. M., Witten, P. E., Baeverfjord, G., Vegusdal, A., Wadsworth, S. and Ruyter, B. (2009). Diets with different n-6/n-3 fatty acid ratio in diets for juvenile Atlantic salmon, effects on growth, body composition, bone development and eicosanoid production. *Aquaculture* **296**, 299-308.
- Bird, N. C. and Mabee, P. M. (2003). Developmental morphology of the axial skeleton of the zebrafish *Danio rerio* (Ostariophysi: Cyprinidae). *Dev. Dyn.* **228**, 337.
- Bloch-Zupan, A. (2016). Hypophosphatasia: diagnosis and clinical signs—a dental surgeon perspective. *Int. J. Paediatr. Dent.* **26**, 426-438.
- Boccaccio, A. and Pappalettere, C. (2011). Mechanobiology of fracture healing: basic principles and applications in orthodontics and orthopaedics. In *Theoretical Biomechanics* (ed. V. Klika), pp. 21-48. London: InTech.
- Boivin, G. and Meunier, P. J. (2002). The degree of mineralization of bone tissue measured by computerized quantitative contact microradiography. *Calc. Tiss. Int.* **70**, 503-511.
- Bruneel, B. and Witten, P. E. (2015). Power and challenges of using zebrafish as a model for skeletal tissue imaging. *Conn. Tiss. Res.* **56**, 161-173.
- Cordell, D., Rosemarin, A., Schröder, J. J. and Smit, A. L. (2011). Towards global phosphorus security: a systems framework for phosphorus recovery and reuse options. *Chemosphere* **84**, 747-758.
- Cubbage, C. C. and Mabee, P. M. (1996). Development of the cranium and paired fins in the zebrafish *Danio rerio* (Ostariophysi, Cyprinidae). *J. Morphol.* **229**, 121-160.
- Currey, J. D. (1999). What determines the bending strength of compact bone? *J. Exp. Biol.* **202**, 2495-2503.
- Currey, J. D. (2003). The many adaptations of bone. *J. Biomech.* **36**, 1487-1495.
- Darias, M. J., Mazurais, D., Koumoundouros, G., Cahu, C. L. and Zambonino-Infante, J. L. (2011). Overview of vitamin D and C requirements in fish and their influence on the skeletal system. *Aquaculture* **315**, 49-60.
- De Clercq, A., Perrott, M. R., Davie, P. S., Preece, M. A., Wybourn, B., Ruff, N., Huysseune, A. and Witten, P. E. (2017). Vertebral column regionalisation in Chinook salmon, *Oncorhynchus tshawytscha*. *J. Anat.* **231**, 500-514.
- Denton, J. E. and Marshall, N. B. (1958). The buoyancy of bathypelagic fishes without a gas-filled swimbladder. *J. Mar. Biol. Ass. U.K.* **37**, 753-767.
- Deschamps, M.-H., Kacem, A., Ventura, R., Courty, G., Haffray, P., Meunier, F. J. and Sire, J.-Y. (2008). Assessment of "discreet" vertebral abnormalities, bone mineralization and bone compactness in farmed rainbow trout. *Aquaculture* **279**, 11-17.
- Fjelldal, P. G., Grotmol, S., Kryvi, H., Gjerdet, N. R., Taranger, G. L., Hansen, T., Porter, M. J. R. and Totland, G. K. (2004). Pinealectomy induces malformation of the spine and reduces the mechanical strength of the vertebrae in Atlantic salmon, *Salmo salar* L. *J. Pineal. Res.* **36**, 132-139.
- Fjelldal, P. G., Nordgarden, U. and Hansen, T. (2007). The mineral content affects vertebral morphology in under-yearling smolt of Atlantic salmon (*Salmo salar* L.). *Aquaculture* **270**, 231-239.
- Fjelldal, P. G., Hansen, T., Breck, O., Sandvik, R., Waagbø, R., Berg, A. and Ørnsrud, R. (2009). Supplementation of dietary minerals during the early seawater phase increase vertebral strength and reduce the prevalence of vertebral deformities in fast-growing under-yearling Atlantic salmon (*Salmo salar* L.) smolt. *Aquacult. Nutr.* **15**, 366-378.
- Fjelldal, P. G., Hansen, T. and Albrektsen, S. (2012a). Inadequate phosphorus nutrition in juvenile Atlantic salmon has a negative effect on long-term bone health. *Aquaculture* **334-337**, 117-123.
- Fjelldal, P. G., Hansen, T., Breck, O., Ørnsrud, R., Lock, E.-J., Waagbø, R., Wargelius, A. and Witten, P. E. (2012b). Vertebral deformities in farmed Atlantic salmon (*Salmo salar* L.) – etiology and pathology. *J. Appl. Ichthyol.* **28**, 433-440.
- Fjelldal, P. G., Lock, E.-J., Hansen, T., Waagbø, R., Wargelius, A., Gil-Martens, L., El-Mowafi, A. and Ørnsrud, R. (2012c). Continuous light induces bone resorption and affects vertebral morphology in Atlantic salmon (*Salmo salar* L.) fed a phosphorous deficient diet. *Aquacult. Nutr.* **18**, 610-619.
- Fjelldal, P. G., Albrektsen, S., Witten, P. E., Fontanillas, R., Nankervis, L., Thomsen, T. H. and Breck, O. (2014). *Beinhelse og fosforbehov i laks: Sluttrapport (Bone health and phosphorus requirements of salmon: final report)*. Rapport fra Havforskningsen, 29-2014. Bergen, Norway.
- Fjelldal, P. G., Hansen, T. J., Lock, E.-J., Wargelius, A., Fraser, T. W. K., Sambras, F., El-Mowafi, A., Albrektsen, S., Waagbø, R. and Ørnsrud, R. (2016). Increased dietary phosphorous prevents vertebral deformities in triploid Atlantic salmon (*Salmo salar* L.). *Aquacult. Nutr.* **22**, 72-90.
- Froese, R. (2006). Cube law, condition factor and weight-length relationships: history, meta-analysis and recommendations. *J. Appl. Ichthyol.* **22**, 241-253.
- Gil-Martens, L., Fjelldal, P. G., Lock, E.-J., Wargelius, A., Wergeland, H., Witten, P. E., Hansen, T., Waagbø, R. and Ørnsrud, R. (2012). Dietary phosphorus does not reduce the risk for spinal deformities in a model of adjuvant-induced inflammation in Atlantic salmon (*Salmo salar*) post-smolts. *Aquacult. Nutr.* **18**, 12-20.
- Gistelinc, C., Kwon, R. Y., Malfait, F., Symoens, S., Harris, M. P., Henke, K., Hawkins, M. B., Fisher, S., Sips, P., Guillemy, B. et al. (2018). Zebrafish type I collagen mutants faithfully recapitulate human type I collagenopathies. *Proc. Natl. Acad. Sci. USA* **115**, E8037-E8046.
- Goetz, R., Nakada, Y., Hu, M. C., Kurosu, H., Wang, L., Nakatani, T., Shi, M., Eliseenkova, A. V., Razzaque, M. S., Moe, O. W. et al. (2010). Isolated C-terminal tail of FGF23 alleviates hypophosphatemia by inhibiting FGF23-FGFR-Klotho complex formation. *Proc. Natl. Acad. Sci. USA* **107**, 407-412.
- Guglielmi, G., Muscarella, S. and Bazzocchi, A. (2011). Integrated imaging approach to osteoporosis: State-of-the-art review and update. *Radiographics* **31**, 1343-1364.
- Günther, A. (1878). II. Preliminary notices of deep-sea fishes collected during the Voyage of H.M.S. 'Challenger'. *Ann. Mag. Nat. Hist.* **2**, 17-28.
- Hamlin, N. J. and Price, P. A. (2004). Mineralization of decalcified bone occurs under cell culture conditions and requires bovine serum but not cells. *Calc. Tiss. Int.* **75**, 231-242.
- Helland, S., Denstadli, V., Witten, P. E., Hjelde, K., Storebakken, T. and Baeverfjord, G. (2006). Occurrence of hyper dense vertebrae in Atlantic salmon (*Salmo salar* L.) fed diets with graded levels of phytic acid. *Aquaculture* **261**, 603-661.
- Hori, M., Shimizu, Y. and Fukumoto, S. (2011). Minireview: fibroblast growth factor 23 in phosphate homeostasis and bone Metabolism. *Endocrinology* **152**, 1-4.
- Huxley, T. H. (1859). Observations on the development of some parts of the skeleton of fishes. *Quart. J. Microsc. Sci.* **7**, 33-46.
- Imsland, A. K., Handeland, S. O. and Stefansson, S. O. (2014). Photoperiod and temperature effects on growth and maturation of pre- and post-smolt Atlantic salmon. *Aquacult. Int.* **22**, 1331-1345.
- Johnston, I. A. (1981). Structure and function of fish muscles. *Symp. Zool. Soc. Lond.* **48**, 71-113.
- Knochel, J. P. (1977). Pathophysiology and clinical characteristics of severe hypophosphatemia. *Arch. Intern. Med.* **137**, 203-220.
- Kvellestad, A., Høie, S., Thorud, K., Tørud, B. and Lyngøy, A. (2000). Platypondyly and shortness of vertebral column in farmed Atlantic salmon *Salmo salar* in Norway – description and interpretation of pathological changes. *Dis. Aquat. Org.* **39**, 97-108.
- Kyle, H. M. (1927). Über die Entstehung und Bildung der Hartschubstanz bei Fischen. *Z. Mikrosk. Anat. Forsch.* **9**, 317-384.
- Laerm, J. (1976). The development, function, and design of amphicoelous vertebrae in teleost fishes. *Zool. J. Linn. Soc.* **58**, 237-254.
- Lock, E.-J., Waagbø, R., Wendelaar Bonga, S. and Flik, G. (2010). The significance of vitamin D for fish: a review. *Aquacult. Nutr.* **16**, 100-116.
- Longo, S., Riccio, M. and McCune, A. R. (2013). Homology of lungs and gas bladders: Insights from arterial vasculature. *J. Morphol.* **274**, 687-703.
- Maisey, J. G. (1991). *Santana Fossils. An Illustrated Atlas*. New York: T.F.H Publications Inc.
- Maisey, J. G. (2000). *Discovering Fossil Fishes*. Boulder, CO: Westview Press.
- National Research Council (2011). *Nutrient Requirements of Fish and Shrimp. Committee on the Nutrient Requirements of Fish and Shrimp*. Washington, DC: The National Academies Press.
- Naylor, R. L., Hardy, R. W., Bureau, D. P., Chiu, A., Elliott, M., Farrell, A. P. I., Forster Gatiin, D. M., Goldberg, R. J., Hua, K. and Nichols, P. D. (2009). Feeding aquaculture in an era of finite resources. *Proc. Natl. Acad. Sci. USA* **106**, 15103-15110.
- Neel, E. A. A., Aljabo, A., Strange, A., Ibrahim, S., Coathup, M., Young, A. M., Bozoc, L. and Mudera, V. (2016). Demineralization–remineralization dynamics in teeth and bone. *Int. J. Nanomed.* **11**, 4743-4763.
- Nordvik, K., Kryvi, H., Totland, G. K. and Grotmol, S. (2005). The salmon vertebral body develops through mineralization of two preformed tissues that are encompassed by two layers of bone. *J. Anat.* **206**, 103-114.
- Pauwels, F. (1960). Einfluss mechanischer Reize auf die Differenzierung der Stützgewebe. *Z. Anat. Entwicklungs.* **121**, 478-515.
- Phleger, C. F. (1988). Bone lipids of jamaican reef fishes. *Comp. Biochem. Physiol.* **90B**, 279-283.
- Poirier Stewart, N., Deschamps, M. H., Witten, P. E., Le Luyer, J., Proulx, E., Huysseune, A., Bureau, D. P. and Vandenberg, G. W. (2014). X-ray-based morphometrics: an approach to diagnose vertebral abnormalities in under-mineralized vertebrae of juvenile triploid all-female rainbow trout (*Oncorhynchus mykiss*) fed with a phosphorus deficient diet. *J. Appl. Ichthyol.* **30**, 496-803.
- Presnell, J. K. and Schreiber, M. P. (1998). *Humason's Animal Tissue Techniques*. Baltimore, MD: The Johns Hopkins University Press.
- Rome, L. C. (2000). Fish as an experimental model to study muscle function. In *The Laboratory Fish* (ed. G. K. Ostrander), pp. 319-300. Baltimore, MD: Academic Press.
- Schmitz, R. J. (1998). Immunohistochemical identification of the cytoskeletal elements in the notochord cells of bony fishes. *J. Morphol.* **236**, 105-116.
- Smedley, M. A., Migaud, H., McStay, E. L., Clarkson, M., Bozzolla, P., Campbell, P. and Taylor, J. F. (2018). Impact of dietary phosphorous in diploid and triploid

- Atlantic salmon (*Salmo salar* L.) with reference to early skeletal development in freshwater. *Aquaculture* **490**, 329-343.
- Sugiura, S. H., Hardy, R. W. and Roberts, R. H.** (2004). The pathology of phosphorus deficiency in fish—a review. *J. Fish Dis.* **27**, 255-265.
- Sullivan, M., Reid, S. W. J., Ternent, H., Manchester, N. J., Roberts, R. J., Stone, D. A. J. and Hardy, R. W.** (2007a). The aetiology of spinal deformity in Atlantic salmon, *Salmo salar* L.: influence of different commercial diets on the incidence and severity of the preclinical condition in salmon parr under two contrasting husbandry regimes. *J. Fish Dis.* **30**, 759-767.
- Sullivan, M., Hammond, G., Roberts, R. J. and Manchester, N. J.** (2007b). Spinal deformation in commercially cultured Atlantic salmon, *Salmo salar* L.: a clinical and radiological study. *J. Fish Dis.* **30**, 745-752.
- Tausky, H. H. and Shorr, E.** (1953). A microcolorimetric method for the determination of inorganic phosphorus. *J. Biol. Chem.* **202**, 675-685.
- Vielma, J. and Lall, S. P.** (1998). Control of phosphorus homeostasis of Atlantic salmon (*Salmo salar*) in fresh water. *Fish Physiol. Biochem.* **19**, 83-93.
- Viguet-Carrin, S., Garnero, P. and Delmas, P. D.** (2006). The role of collagen in bone strength. *Osteoporosis Int.* **17**, 319-336.
- Weinans, H. and Prendergast, P. J.** (1996). Tissue adaptation as a dynamical process far from equilibrium. *Bone* **19**, 143-149.
- Weisberg, P., Scanlon, K. S., Li, R. and Cogswell, M. E.** (2004). Nutritional rickets among children in the United States: review of cases reported between 1986 and 2003. *Am. J. Clin. Nutr.* **80**, 1697S-1705S.
- Wilton, T. J., Hosking, D. J., Pawley, E., Stevens, A. and Harway, L.** (1987). Osteomalacia and femoral neck fractures in the elderly patient. *J. Bone Joint Surg.* **69B**, 388-390.
- Witten, P. E. and Hall, B. K.** (2002). Differentiation and growth of kype skeletal tissues in anadromous male Atlantic salmon (*Salmo salar*). *Int. J. Dev. Biol.* **46**, 719-730.
- Witten, P. E. and Huysseune, A.** (2009). A comparative view on mechanisms and functions of skeletal remodelling in teleost fish, with special emphasis on osteoclasts and their function. *Biol. Rev.* **84**, 315-346.
- Witten, P. E., Gil-Martens, L., Hall, B. K., Huysseune, A. and Obach, A.** (2005). Compressed vertebrae in Atlantic salmon (*Salmo salar*): evidence for metaplastic chondrogenesis as a skeletogenic response late in ontogeny. *Dis. Aquat. Org.* **64**, 237-246.
- Witten, P. E., Obach, A., Huysseune, A. and Baeverfjord, G.** (2006). Vertebrae fusion in Atlantic salmon (*Salmo salar*), Development, aggravation and pathways of containment. *Aquaculture* **258**, 164-172.
- Witten, P. E., Gil-Martens, L., Huysseune, A., Takle, H. and Hjelde, K.** (2009). Towards a classification and an understanding of developmental relationships of vertebral body malformations in Atlantic salmon (*Salmo salar* L.). *Aquaculture* **295**, 6-14.
- Witten, P. E., Owen, M. A. G., Fontanillas, R., Soenens, M., McGurk, C. and Obach, A.** (2016). Primary P-deficiency in juvenile Atlantic salmon: the uncoupling of bone formation and mineralisation. *J. Fish Biol.* **88**, 690-708.
- Witten, P. E., Harris, M. P., Huysseune, A. and Winkler, C.** (2017). Small teleost fish provide new insights into human skeletal diseases. *Methods Cell Biol.* **138**, 321-344.
- Ytteborg, E., Torgersen, J. S., Pedersen, M. E., Baeverfjord, G., Hannesson, K. O. and Takle, H.** (2010). Remodeling of the notochord during development of vertebral fusions in Atlantic salmon (*Salmo salar*). *Cell Tiss. Res.* **342**, 363-376.

**Table S1. Diet composition**

Ingredient (%)	High phosphorus (HP)	Normal phosphorus (RP)	Low phosphorus (LP)
Wheat <sup>1</sup>	17.2	17.9	19.5
Wheat gluten <sup>1</sup>	23.6	23.5	23.3
Soy protein concentrate <sup>2</sup>	23.0	23.0	23.0
Fish meal <sup>3</sup>	10.0	10.0	10.0
Fish oil <sup>3</sup>	22.3	22.3	22.2
Inorganic phosphate <sup>4</sup>	2.0	1.4	0.0
Vitamin/mineral/ amino acid mix <sup>4</sup>	1.93	1.94	1.96
<i>Total Phosphorus in diet</i>	<i>1.46%</i>	<i>0.84%</i>	<i>0.49%</i>

<sup>1</sup> Skretting Norway, Stavanger, Norway.

<sup>2</sup> Imcopa, Rotterdam, Netherlands.

<sup>3</sup> North Atlantic fishmeal and oil, Skretting Norway, Stavanger, Norway.

<sup>4</sup> Trouw Nutrition International, Nijverheidsweg 2, 3881 LA, Putten. The Netherlands. Premixes formulated to meet all NRC (2011) requirements for salmonids excluding phosphorus.



**Table S2. Growth parameters of animals fed with a requirement phosphorus (RP) or low phosphorus (LP) diet for the experimental periods.**

Experimental Period	Diet Group	Weight in g	Fork Length	Specific Growth Rate	Feed Conversion Rate	Condition Factor
sampling after 7 weeks (intermediate sampling)	RP	340.3±05.7 <sub>a</sub>	29.64±0.06 <sub>a</sub>	1.70±0.04 <sup>a</sup>	0.62±0.01 <sup>a</sup>	1.25±0.09
	LP	286.4±08.7 <sub>b</sub>	27.62±0.12 <sub>b</sub>	1.33±0.06 <sup>b</sup>	0.73±0.03 <sup>b</sup>	1.37±0.13
sampling after 16 weeks (final sampling)	RP-RP	702.9±40.4 <sub>x</sub>	37.07±0.56 <sub>x</sub>	1.21±0.10 <sup>xy</sup>	0.75±0.03	1.38±0.05
	LP-LP	558.7±16.3 <sub>y</sub>	34.11±0.09 <sub>y</sub>	1.09±0.06 <sup>x</sup>	0.78±0.12	1.39±0.03
	LP-RP	604.4±05.2 <sub>xy</sub>	35.26±0.02 <sub>xy</sub>	1.31±0.02 <sup>xy</sup>	0.65±0.00	1.36±0.00
	LP-HP	678.3±42.9 <sub>xy</sub>	36.14±1.18 <sub>xy</sub>	1.42±0.05 <sup>y</sup>	0.67±0.00	1.47±0.11

Statistics: All values are means ± standard deviation of the tank average. Where appropriate the differences between groups was analyzed either by Students T-test (for two groups at the intermediate sampling point), or ANOVA (for 4 groups in the final sampling). Different superscripts (a,b,x,y) in the same column indicate significant differences ( $P < 0.05$ ) with each sampling point compared independently.

**Table S3. Biomechanical testing.** Vertebra stiffness ( $\text{Nmm}^{-1}$ ) in Atlantic salmon post-smolts in seawater fed diets with low (LP) or regular (RP) phosphorus contents for 7 weeks, and then the fish previously fed the LP diet were shifted to diets with low (LP-LP), regular (LP-RP), or high (LP-HP) phosphorus contents for 9 weeks. The fish previously fed the RP diet was fed further on this diet for the same time period. The data are from the terminal sampling after 16 weeks of feeding. Values are expressed as mean $\pm$ SE. Different lower case letters denotes significant differences (SNK,  $P < 0.05$ ). N = number of animals analyzed.

	Group				P-value
	RP-RP	LP-LP	LP-RP	LP-HP	
Stiffness ( $\text{Nmm}^{-1}$ )	198.5 $\pm$ 15.4a	59.2 $\pm$ 4.2c	154.3 $\pm$ 14.6b	203.8 $\pm$ 8.2a	0.00018
N	15	10	10	10	